Experimental Characterization of Plasma Heating with Beating Electrostatic Waves

Benjamin Jorns* and Edgar Y. Choueiri†

Electric Propulsion and Plasma Dynamics Laboratory, Princeton University, Princeton, NJ, 08540

The heating of ions in a magnetized plasma by two electrostatic waves whose frequencies differ by the ion cyclotron frequency is experimentally and analytically characterized. An analytical model is presented for the power absorption by the two waves, and it is shown that the two-wave process will yield superior heating to a single electrostatic wave only in the event that the total wave energy density exceeds a threshold value. An experimental investigation of the increase in ion temperature as a function of the fraction of total energy density in one of the propagating modes subsequently reveals that for a low temperature plasma, heating with a single electrostatic wave is superior to employing two beating electrostatic waves. This result is consistent with the analytical prediction that the available wave energy density in the experiment is below the required threshold for the superiority of the two-wave process.

I. Introduction

The heating of plasmas with externally coupled radiofrequency (RF) waves is a critical process for applications across the spectrum of plasma science. This stems from the ability of RF waves to introduce energy without directly contacting the plasma—an attractive feature for applications where efficiency and material erosion considerations are paramount. For plasma propulsion in particular where thruster lifetime is largely limited by the erosion of the materials exposed to the plasma, electrodelessly coupling energy to the exhaust with RF waves is an important alternative method for efficiently producing continuous thrust.

With these apparent advantages in mind, there a number of propulsion applications that depend on inductively coupling coherent plasma wave modes into the propellant.[1–4] All of these proposed concepts rely on a magnetic field for plasma confinement, and as a consequence, when the thrust is directed along this field, magnetic detachment becomes a significant concern. In order to circumvent this issue, we proposed in 2010 and 2011 two concepts that provide transverse acceleration across the confining magnetic field.[5,6] This end is accomplished in both of these proposed concepts by coupling to a plasma mode that propagates across a uniform region of magnetic field.

For these concepts relying on transverse mode propagation, it is desirable to energize as much of the ion population in the plasma as possible. One candidate mode to achieve this end is an obliquely propagating electrostatic wave that exists near the ion cyclotron frequency. As this wave traverses the plasma, it deposits power in the ions through a resonant mechanism—a process where only a subset of particles with appropriately conditioned parallel velocities will interact with the wave. For low-frequency, obliquely propagating electrostatic modes, this resonant condition can be expressed in terms of the ion velocity and ion cyclotron frequency,[7] $\omega - k_z v_z - n\Omega_i = 0$ where ω denotes the wave frequency, v_z denotes the parallel velocity of ions, k_z is the parallel velocity of the wave, Ω_i is the ion cyclotron frequency, and n is an integer. This resonant condition is accompanied by a similar requirement on the perpendicular velocity of the waves, $\omega/k_\perp < v_\perp$ where $k_\perp$ denotes the perpendicular wavenumber. This resonant process for energy exchange with the wave, commonly referred to as ion cyclotron and ion cyclotron harmonic heating, can be quite efficient for plasmas where the majority of particles satisfy the resonant condition. For relatively low temperature plasmas, however, where the phase velocity of the wave in both directions is significantly larger than the average thermal velocity of the ensemble, $v_{th(i)} \ll \omega/k_{||}, \omega/k_\perp$, the resonant condition will only be

*Graduate Researcher

†Chief Scientist, EPPDyL, Professor, Applied Physics Group, MAE Dept.

satisfied for waves that are *on-resonance*, i.e. with a frequency that is an integer multiple of the ion cyclotron frequency. Moreover, due to the condition for phase velocity in the perpendicular direction, even in the case of on-resonance frequency, only a few ions in the tail of thermalized ensemble distribution will satisfy the perpendicular resonant condition. This restriction can significantly limit the energy exchange with a single electrostatic wave (SEW).

One way to overcome this issue is to employ waves with lower phase velocities relative to the thermal velocity, however, for the common case where the wave phase velocity has a lower bound (imposed by a dispersion relation), the SEW process will have limited efficiency. In light of this limited range in wave phase velocity, a number of authors[8,11,13] have proposed a nonlinear mechanism to non-resonantly target the low energy ions with velocities well outside the resonant conditions for SEW. In particular, when two electrostatic waves (BEW) are launched in the plasma that satisfy the so-called beat condition, $\omega_2 - \omega_1 = n\Omega_i$ where n is an integer, the interaction of the two modes gives rise to a beat wave at the difference frequency $\omega' = \omega_2 - \omega_1$ and wavenumber $\mathbf{k}_2 - \mathbf{k}_1$. This beat mode targets low energy ions since it has a frequency that automatically is on-resonance, $\omega' = \Omega_i$, and depending on the dispersion relation of the exciting electrostatic modes, this driven mode also can have a lower phase velocity than the individual SEW. As a result, the non-linear beat wave can effectively couple energy to ions whose initial velocities do not satisfy the resonant condition for SEW.

Given the apparent advantages of employing two waves over a single wave in low temperature plasmas, a large body of work has developed on the beating wave interaction. This work has proceeded on two fronts–separated both by time and approach. Porkolab and Chang[8] in the 1970s were the first to examine analytically the beating wave effect for obliquely propagating modes in a magnetized plasma. Their work was reproduced from an elegant consideration of the oscillation center formulation by Johnston.[9] In both of these investigations, the BEW effect was examined self-consistently from the Vlasov and Poisson equations, and terms for power deposition were derived under the assumption of the random phase approximation. Chang and Porkolab subsequently were able to confirm experimentally their predicted model for the power deposition caused by the beat wave.[10]

In more recent years, a number of analyses based on single particle dynamics have been done in order to characterize the response of a single particle to the trajectory.[11–16] That research developed in response to a need to explain anomalous acceleration of ions in the earth's ionosphere[11] where the particle densities are so low that a single particle description is justified. The advantage of this treatment is that it permits a characterization of the small timescale dynamics of BEW acceleration. Indeed, these studies have resulted in a greater understanding of how the beat mode interacts with individual ions.[13,14,16] One of the more important results that stemmed from that work is the demonstration that the onset of heating occurs for BEW at lower total energy density than for the case of SEW heating.[17,18]

The combination of kinetic formulation and single particle analysis thus have provided a full description of when heating occurs with BEW and how the power is deposited in the plasma ions. In the context of our motivation to more efficiently heat plasmas, these tools permit us to pose the central question: is BEW heating superior to SEW heating? Our first analytical investigation into this question in 2011 showed that for the special case of equal wave amplitudes and wavenumbers, BEW was the superior process.[19] However, the equal wavenumber assumption of this model is questionable when considering real plasma wave dispersion relations, and it was necessary to introduce an ad hoc correction to account for the energy exchange with the beat mode. There consequently remained some analytical ambiguity as to whether or not the BEW process is superior. Experimental investigations into the superiority of BEW heating (BEWH) similarly were extremely limited in scope.[20,21]

The need is apparent for a more rigorous investigation into the superiority of BEWH, and the goal of this work is to accomplish this analysis both analytically and experimentally. With this end in mind, this paper is organized in the following way. In the first section, we review the predicted characteristics of BEW and establish a criterion for when BEW power deposition is superior to SEW deposition. In the second section, we describe the Beating Waves Experiment II (BWX II) and the diagnostics for determining wave properties and temperature increase in the plasma. In the third section, we present an experimental characterization of SEW propagation and plasma heating and use these data to select a frequency pair for experimental investigation with BEW. In the fourth section, we present a parametric investigation of plasma heating in BWX II with two BEW. And in the fifth and final section, we discuss the implications of our results for both plasma heating and plasma propulsion.

II. Power absorption by beating electrostatic waves

We assume that the wave amplitudes of the two waves are sufficiently large that the onset of heating has occurred (this is beyond the range of the experimental results of Ref. 18 where these threshold effects were examined). In this case of large amplitude, particle orbits are sufficiently de-correlated to permit a random phase approximation such that the power absorption for the BEW process is given by (c.f. Refs. 8, 22, 23):

$$P_d = \alpha_1 \Phi_1^2 + \alpha_2 \Phi_2^2 + \Phi_1^2 \Phi_2^2 \gamma_{12}, \tag{1}$$

where Φ_j denotes the potential amplitude of the propagating modes, α_j is a coefficient that corresponds to the single wave absorption process, and γ_{12} is a factor that scales with the nonlinear, BEW absorption that arises from the beat term at the difference frequency $\omega' = \omega_2 - \omega_1$. We note that the α_j depend on the absorption process, and in the limit of SEW propagation, we see that the nonlinear term disappears.

For our analysis, we compare the SEW process with the BEW process under the condition that each has the same total wave energy density, W_T. For the case of two propagating modes, this quantity is given by

$$W_T = \beta_1 \Phi_1^2 + \beta_2 \Phi_2^2 \tag{2}$$

where β_j is the coupling coefficient that depends on the dispersion relation of the propagating mode. In order to simplify our analysis further, we define the fraction of the total energy in the first wave as

$$\eta = \frac{\beta_1 \Phi_1^2}{W_T}. \tag{3}$$

such that we have

$$\begin{aligned} \Phi_1^2 &= \frac{\eta}{\beta_1} W_T \\ \Phi_2^2 &= \frac{W_T}{\beta_2} (1 - \eta). \end{aligned} \tag{4}$$

Substituting these expressions into Eq. 1, we thus find

$$P_d = W_T \left(\frac{\alpha_1}{\beta_1} \eta + \frac{\alpha_2}{\beta_2} (1 - \eta) + W_T \frac{\gamma_{12}}{\beta_1 \beta_2} \eta (1 - \eta) \right). \tag{5}$$

This result expresses the total power deposition in the plasma due to the BEW effect as a function of the fraction of the total energy density in the first mode. It permits us to formulate a simple criterion for the case where BEW is superior to SEW. Specifically, if BEW produces superior heating to SEW (where $\eta = 0$ or 1), then for the same total energy density, there should be some combination of the two waves where the increase in ion temperature for BEW is greater than the equivalent temperature increase at either SEW frequency. More succinctly, if we define $F(\eta) = [T_i(\eta) - T_{i0}] / T_{i0}$, the fractional increase in ion temperature T_i due to wave heating, then if BEW is the more efficient process for fixed W_T, there exists a range of $\eta \in (0, 1)$ such that $F(\eta) > F(0), F(1)$.

Since P_d is a smoothly varying function, we see that this requirement for the superiority of BEW can be translated into calculating the optimal value of η:

$$\eta = \frac{1}{2} + \frac{\alpha_1 \alpha_2}{2 \gamma_{12} W_T} \left(\frac{\beta_2}{\alpha_2} - \frac{\beta_1}{\alpha_1} \right). \tag{6}$$

This result is physically intuitive. For increasing total energy density or a larger nonlinear coupling term, we see that the optimal value approaches an equal split between the two density modes. We further can see from this criterion that in order for BEW to be the more efficient process (where $\eta \in (0, 1)$), it is necessary that

$$W_T > W_T^* \equiv \left| \frac{\alpha_1 \alpha_2}{\gamma_{12}} \left(\frac{\beta_2}{\alpha_2} - \frac{\beta_1}{\alpha_1} \right) \right|. \tag{7}$$

In other words, there is a threshold value, W_T^*, for total wave energy density for the BEW process to be superior to SEW. This threshold reflects the higher order dependence of the nonlinear cross term (proportional to γ_{12}) in Eq. 1. The interesting consequence of this expression is that while BEW is always the superior process for sufficiently large input energy, at low wave energies this advantage can disappear. For experiments and applications where the input power to the waves is limited, it may be possible that it is preferable to employ SEW. A discussion of the coefficients and their dependence on wave and plasma parameters becomes particularly important in such cases, and in the next section we summarize these coefficients for the physically applicable case of obliquely propagating electrostatic waves in a low temperature plasma.

Ion Cyclotron Harmonic Damping

For the case of electrostatic modes with finite parallel wavenumbers in a uniform magnetic field, the classic mechanism for power absorption by the ions is ion cyclotron harmonic damping (cf. 7, 24). This occurs primarily for ions that satisfy the resonant condition $\omega - k_z v_z - n\Omega_i = 0$, which can be interpreted as giving the velocity where the particle's Larmor precession maintains a constant phase with respect to the wave's electric field in the plane normal to magnetic field. Direct energy exchange occurs under these circumstances. From a kinetic perspective, the coefficients α_1 and α_2 for this process can be derived from the first-order components of the anti-Hermitian, kinetic susceptibility tensor.[7] The nonlinear term, γ_{12}, on the other hand can be found from a Hamiltonian formulation for power deposition[9] or a fourth order expansion of the Vlasov equation.[8]

With this in mind, for electrostatic waves with an isotropic background temperature T_{i0} and drift velocity V in the parallel direction, the coefficient for absorption is given by[7]

$$\alpha_j = \pi n_0 m_i \Omega_i^2 \left(\frac{1}{B_0}\right)^2 \sum_n \mathrm{Im}\left[\int_0^\infty \int_{-\infty}^\infty v_\perp dv_\perp dv_z \frac{J_n^2(z_j)\left(k_z \frac{\partial f_0}{\partial v_z} + n\frac{\Omega_i}{v_\perp}\frac{\partial f_0}{\partial v_\perp}\right)(n\Omega_i + v_z k_{zj})}{(n\Omega_i + k_{zj} v_z - \omega_j)}\right], \quad (8)$$

where we have defined $z_j = k_j v_\perp / \Omega_i$, n_0 is the plasma density, q is the charge, and m_i denotes the ion mass. We evaluate the velocity integral in the parallel direction with the Plemelj relationship:

$$\alpha_j = \frac{\pi^2 n_0 m_i \Omega_i^2}{k_{zj}} \left(\frac{1}{B_0}\right)^2 \sum_n \int_0^\infty \int_{-\infty}^\infty v_\perp dv_\perp dv_z J_n^2(z_j)\left(k_z \frac{\partial f_0}{\partial v_z} + n\frac{\Omega_i}{v_\perp}\frac{\partial f_0}{\partial v_\perp}\right)(n\Omega_i + v_z k_{zj})\,\delta\left(v_z - \frac{\omega_j - n\Omega_i}{k_{zj}}\right). \quad (9)$$

We then apply the delta function to yield the simplified result:

$$\alpha_j = n_0 m_i \left(\frac{m_i}{T_{i0}}\right)^{3/2} \frac{\pi^2 \Omega_i^2}{\sqrt{2\pi} k_{zj}} \left(\frac{1}{B_0}\right)^2 \omega_j(\omega_j - k_{zj} V) \sum_n e^{-m_i(\omega_j - n\Omega_i - k_{zj}V)^2/2k_{zj}^2 T_{i0}} \int_0^\infty v_\perp dv_\perp J_n^2(z_j) f_\perp^{(0)}, \quad (10)$$

where we have assumed a perpendicular thermal distribution given by

$$f_\perp^{(0)} = \left(\frac{m}{2\pi T_{i0}}\right) e^{-m_i v_\perp^2/2T_{i0}}. \quad (11)$$

Using a Bessel function identity from Ref. 25 (p. 395) we can simplify this result further to a compact expression for ion cyclotron damping,

$$\alpha_j = n_0 m \pi^2 \Omega_i^2 k_{zj}^{-1} \left(\frac{1}{B_0}\right)^2 \left(\frac{m_i}{2\pi T_{i0}}\right)^{3/2} \omega_j(\omega_j - k_{zj}V)\, e^{-\lambda_j} \sum_n I_n(\lambda_j)\, e^{-m_i(\omega_j - n\Omega_i - k_{zj}V)^2/2T_{i0}k_{zj}^2}, \quad (12)$$

where we have defined $\lambda_j = T_{i0}/m_i (k_{\perp j}/\Omega_i)^2$.

The nonlinear term can be derived either from a consideration of the perturbations to the Vlasov equation or from a kinetic formulation. We present here a simplified form:[9]

$$\gamma_{12} = n_0 m_i \frac{\pi^2}{\sqrt{2\pi}\Delta k_z}\left(\frac{m_i}{T_{i0}}\right)^{3/2}\left(\frac{\Omega_i}{B_0}\right)^4 \Delta\omega\left(\Delta\omega - \Delta k_z V\right) e^{-m_i(\Delta\omega - \Delta k_z V - p\Omega_i)/2T_{i0}(\Delta k_z)^2} \times \sum_{p,m}\int_{-\infty}^{\infty}\int_{0}^{\infty} v_\perp dv_\perp dv_z A_p^m A_p^n f_\perp^{(0)}\delta\left(v_z - \frac{\Delta\omega - p\Omega_i}{\Delta k_z}\right), \tag{13}$$

where we have defined $\Delta k = k_{z2} - k_{z1}$, $\Delta\omega = \omega_2 - \omega_1$, and the velocity-dependent terms

$$\begin{aligned} A_p^m =& \frac{1}{4}\left(k_{1z}k_{2z}J_m\left(z_1\right)J_{m+p}\left(z_2\right)\left[\frac{\left(1-\mathfrak{D}_2^{m+p}\right)}{\left[\left(m+p\right)\Omega_i + v_z k_{z2} - \omega_2\right]^2} + \frac{\left(1-\mathfrak{D}_1^{m}\right)}{\left[m\Omega_i + v_z k_{z1} - \omega_1\right]^2}\right]\right. \\ &+ m\frac{\Omega_i}{v_\perp}\left[J_m\left(z_2\right)J'_{m-p}\left(z_1\right)\left(\frac{\left(1-\mathfrak{D}_2^{m-p}\right)}{\left(m-p\right)\Omega_i + v_z k_{z1} - \omega_1} + \frac{\left(1-\mathfrak{D}_2^{m}\right)}{m\Omega_i + v_z k_{z2} - \omega_2}\right)\right. \\ &\left.\left. + J_m\left(z_1\right)J'_{m+p}\left(z_2\right)\left(\frac{\left(1-\mathfrak{D}_1^{m}\right)}{m\Omega_i + v_z k_{z1} - \omega_1} + \frac{\left(1-\mathfrak{D}_2^{m+p}\right)}{\left(m+p\right)\Omega_i + v_z k_{z2} - \omega_2}\right)\right]\right). \end{aligned} \tag{14}$$

Here we have defined $\mathfrak{D}$ as a narrow filter[9] that picks out the resonant terms at $\omega_j - n\Omega_i - k_{zj}v_z$, which we approximate as

$$\mathfrak{D}\left(x\right) = \lim_{h\to\infty}\sqcap\left(h\left[\frac{1}{2} - x\right]\right), \tag{15}$$

where $\sqcap$ denotes the Boxcar function. This term eliminates the secularities associated with the single wave resonances.

Finally, we examine the wave energy density coefficients. Following Stix,[7] we use the traditional definition of energy density to find for each propagating mode:

$$\beta_j = \epsilon_0\frac{\omega_i}{4}\frac{\partial}{\partial\omega_i}D\left(\mathbf{k}_i, \omega_i\right) \tag{16}$$

where ϵ_0 is the permittivity of free space and D is the electrostatic dispersion relation for an isotropic plasma given by

$$D\left(\mathbf{k},\omega\right) = k_{||}^2 + k_\perp^2 + \sum_{s=e,i}k_{ds}^2\left(1 + \sum_n e^{-a_s}I_n\left(a_s\right)Z\left(\zeta_n\right)\left(\zeta_n + \frac{n\Omega}{\sqrt{2}k_z v_{th}}\right)\right). \tag{17}$$

where we have defined $\zeta_n = \left(\omega - n\Omega_s - k_z V_s\right)/\sqrt{2}v_{th}$; the thermal velocity, $v_{th(s)}^2 = T_{s0}/M_s$; the plasma dispersion function, $Z\left(\zeta_n\right) = 1/\sqrt{\pi}\int_{-\infty}^{\infty}\left[e^{-s^2}/\left(s-\zeta_n\right)\right]ds$; $a_s = \left(k_\perp\rho_s\right)^2$; $\rho_s = v_{th(s)}/\Omega_s$; V_s is the drift velocity of the given species; and I_n is the modified Bessel function of the first kind.

With these coefficients, if we know the plasma and wave parameters, we can determine from Eq. 7 the minimum wave energy density required for BEWH to become the superior process. In the next section, we experimentally determine these properties for BWX II and use the above discussion to identify the parameter set with the minimum threshold value for W_T.

III. Experimental setup

For this experimental investigation, we employed an axially symmetric, uniformly magnetized plasma sustained by an inductive, RF discharge. The magnetic field used for our heating measurements was 525 G ($f_{ci} \approx 20$ kHz) while the plasma source was operated in an inductive mode at 275 W with a fill pressure of argon measured at 0.1-1 mT. This yielded an azimuthal density profile with a peak value of the order of 10^{11} cm^{-3} and an electron temperature of approximately $T_e \approx 4$ eV. A more detailed description of the experiment is provided Refs. 26 and 21. A full characterization of the experimental setup shown in Fig. 1. We include here a brief overview of the different elements in the setup.

A. Vacuum chamber and solenoid

We employ a Pyrex cylinder 132 cm in length with a 16.5 cm inner diameter placed concentrically in a 122 cm long, 10 ring solenoid. A small window at the end of the chamber provides longitudinal optical access while argon gas flows into the chamber through a feed in the cross at the opposite end of the chamber. A constant pressure of 0.1 mT is maintained by a 140 l/s turbo pump backed with a roughing pump. The RF plasma source and plasma heating regions are located on opposite sides of the vacuum vessel in order minimize stray RF noise in the experimental region. We chose Pyrex for our vacuum since its low conductivity permits inductive coupling from an external antenna through the wall. The optically transparent vacuum vessel similarly provides optical access over the entire length of the heating zone.

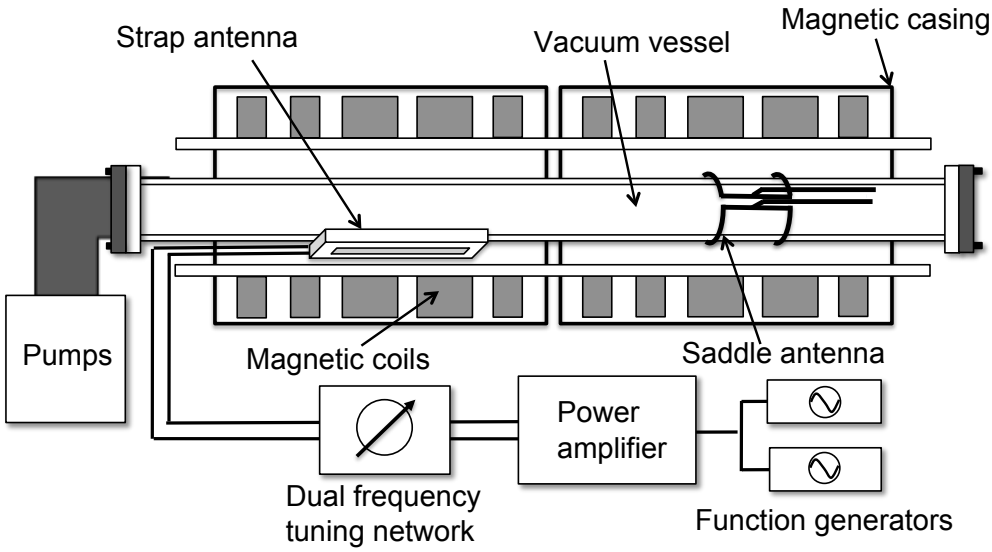

(a) Schematic of the experimental apparatus with the heating antenna matching network.

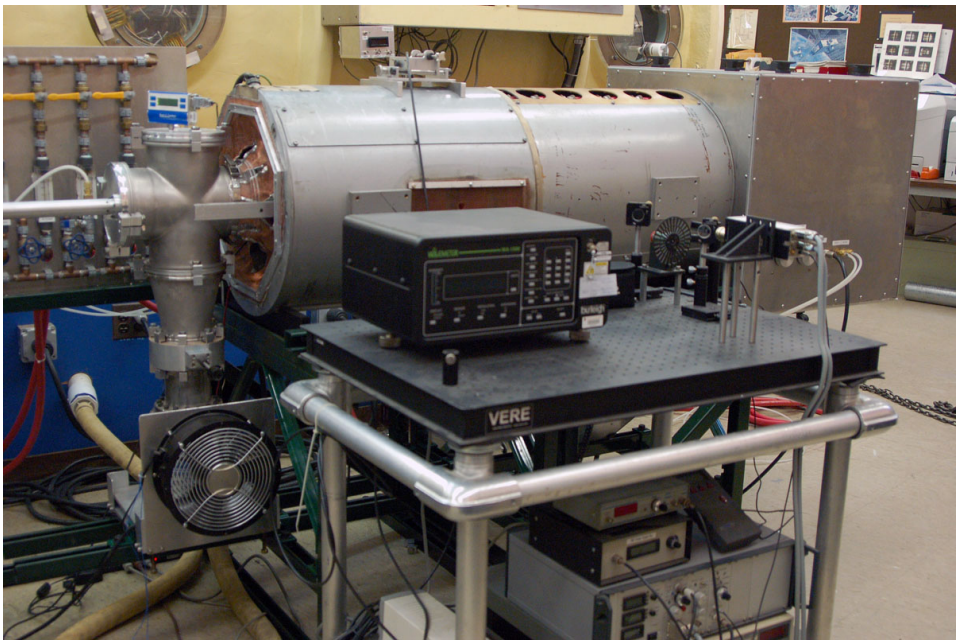

(b) Photograph of the experimental apparatus showing the LIF system in the foreground.

Figure 1. Schematic of the experimental apparatus.

Two klystron Varian 1955A magnets placed end to end provide a magnetic field in the experimental test region. Each magnet has been calibrated experimentally as well as numerically modeled to produce a

uniform field in the experimental region with a magnitude of 525 ±2.5 G. The plasma discharge propagates along the magnetic field lines generated by the solenoid into the uniform-field experimental region.

B. Plasma source

The plasma discharge is produced by a Boswell-type saddle antenna with a 7.25" inner diameter placed around the vacuum chamber at one end of the solenoid. The antenna is powered by a 1.25 kW source operated at 13.56 MHz and matched to the plasma with an L network consisting of two Jennings 1000 pF 3kV variable vacuum capacitors. In order to minimize RF noise from this antenna as well as provide a low energy background for contrast to the heating, we operated this antenna in the inductive mode at 275 W.

C. Wave launching

The waves are launched in this experiment by means of a strap antenna with 40 turns, 5.5 cm in width and 25 cm in length oriented along the plasma axis. This strap configuration is located outside the vacuum vessel and couples to electrostatic modes through the induced electric field in the axial direction that results from the varying magnetic field of the antenna. The space charge that arises to counteract this electric field also produces a significant perpendicular component of the electric field oriented normal to the antenna surface.[27] We employ a planar geometry for the antenna in order to excite approximately planar modes across the center line of the experiment in one direction. This provides for more control in comparing the experimental results to theoretical predictions that were derived under the assumption of planar modes in a Cartesian geometry.

Power is coupled into the electrostatic waves launched from the antenna by means of an ENI 1140 LA amplifier that is matched to the antenna's inductive load by means of the custom designed Variable Dual Frequency Matching network.[28] This provides near optimized matching over the frequency range of interest in this investigation, $f = f_{ci} - 5f_{ci} = 20 - 100$ kHz. The maximum current excited in each mode is 22 A –the point where excessive heating of the matching network by resistive losses significantly changes the matching characteristics. The power output form the amplifier at this point is 400 W.

D. Plasma parameters

The electron temperature, which was measured with an array of double Langmuir probes, was found to be approximately uniform over the majority of the heating volume with $T_e \approx 4$ eV. We observed a small increase in temperature at the plasma edge, which is consistent with cylindrical inductively coupled sources.[29] A

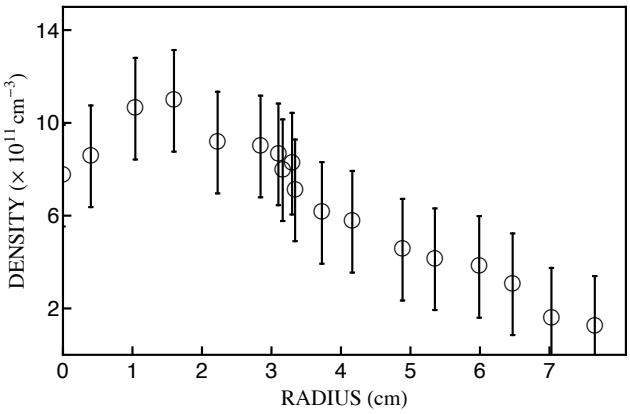

Figure 2. Characteristic radial profile for plasma density in the BWX II heating volume.

typical density profile for the operating conditions of BWX II is shown in Fig. 2. As can be seen, there is an approximately uniform region of density near the center of the plasma with a small dip at $r = 0$. This same trend has been reported for similar inductive discharges at low power.[30] The axial dependence of both temperature and density was found to be uniform for the length of the heating volume.

E. Laser-induced fluorescence

The primary diagnostic for BWX II is a Laser-Induced Fluorescence (LIF) system that is tuned to the $3d^4F_{7/2} - -4p^4D^0_{5/2}$ transition of an AR II metastable line. This tool probes the velocity distribution of ions in the system and provides information both on the ion temperature as well as the dielectric response of the ions to propagating plasma modes.[31,32] The LIF technique is an inherently non-invasive diagnostic for examining ion temperature and wave properties. This is a significant advantage since the kinetic BEW effect can be perturbed by placing probes in the plasma.

The LIF system for BWX II is capable of scanning the velocity profile in both the parallel and perpendicular directions. For temperature measurements, the background velocity distribution is sampled to yield an estimate for T_{i0}. For wave measurements, a Stanford Research 830 lock-in amplifier is employed at the frequency of the propagating wave of interest in order to isolate the signal from the ion oscillations. In this way, the LIF system is capable of measuring the dielectric response of the plasma ions to the electrostatic modes. Through the fitting procedure outlined in Refs. 31 and 32, we were able to use this technique to estimate the local wavenumber of the propagating mode as well as the potential amplitude. All local measurements reported here were performed 3 cm from the center of the plasma column and along the diameter intersecting the strap antenna.

IV. Experimental characterization of SEW

A. Temperature increase with antenna current

In Fig. 3, we show the steady-state ion temperature, T_i as a function of current to the BWX II antenna for the case where two beating waves are employed. Three representative curves are shown for two waves that satisfy $\omega_1 = 2\Omega_i, \omega_2 = 2\Omega_i$ with antenna currents given by I_1 and I_2. We see that each curve exhibits the same qualitative behavior, which can be divided into three regions. At the first transition, the ion temperature experiences a jump above background. This suggests the onset of a stochastic transition, the origin and study of which were the subject of a number of investigations.[17,18] It is this stochastic transition that facilitates the energy exchange of the waves with the plasma. In the second region, there is a nonlinear increase in ion temperature with antenna current. And finally, in the third region, the ion temperature approaches an asymptotic value, typical of saturation.

The saturation behavior in these measurements suggests that there is an equilibrium reached between the power deposition introduced to the ions by the exciting modes to the ions and competing loss mechanisms such as collisional diffusion or parametric decay that prevent further energy from being deposited to the ions. The asymptote with current is an indication where the loss processes become dominant, but since the level of the plateau clearly depends on the current configuration as well as the wave parameters, we use this the asymptotic value as a metric for the efficacy of heating when performing a frequency characterization of SEW heating (where $I_2 = 0$)

B. SEW heating

For our first round of experiments, we examined the frequency dependence of ion heating with a single electrostatic mode ($I_2 = 0$). We accomplished this end by increasing the current to the antenna for each wave frequency and observing the ion temperature in the asymptotic region. We then recorded the fractional increase in ion temperature over background as a function of frequency as shown in Fig. 4. Each value in these plots indicates the maximal heating that could be achieved at that frequency set before competing losses dominated.

As we can see from Fig 4 there is a clear dependence of the ion temperature on the frequency of the propagating modes with an optimal frequency at the second harmonic $\omega = 2\Omega_i$. This optimum lends support to the notion this is an example of ion cyclotron harmonic damping since this process exhibits maximal heating at the ion cyclotron harmonics. We note that there is no peak at the fundamental frequency as the dispersion relation experiences a cut off at this point.

C. Dispersion relation

Using the prescription outlined above for employing LIF to perform wave measurements, we were able to measure a dispersion relation for the modes in the plasma. These measurements were performed at $r = 3$ cm

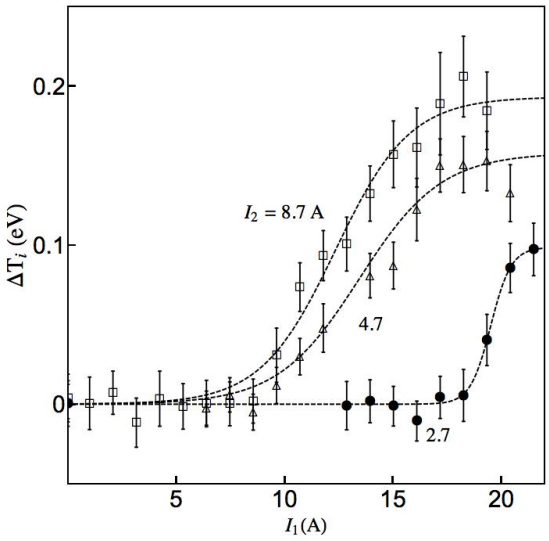

Figure 3. Change in ion temperature as a function of input current I_1 to the lower frequency mode. Each curve corresponds to a fixed level of current in the second mode, I_2.

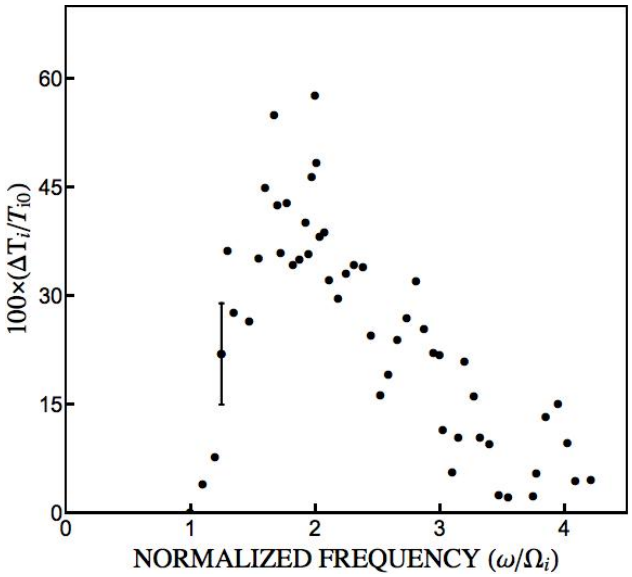

Figure 4. The maximum change ion temperature achieved at each frequency for the SEW case. A representative error bar is shown as well.

where the plasma properties are relatively uniform. The results for the perpendicular component are shown in Fig. 5 along with a representative error bar.

This near-acoustic relationship with a cutoff at the cyclotron frequency suggests that the propagating mode is the electrostatic ion cyclotron wave where the parallel wavenumber is related to the measured perpendicular values through the electrostatic dispersion relation given by Eq. 17. From our measurements, we further have confirmed that the transverse component of the wave vector was oriented normal to the antenna loop. Coupled with the observation that the antenna cross-section presented to the plasma is large, we used the observation of normal approximation from the antenna to confirm that the modes were approximately planar at the area of observation.

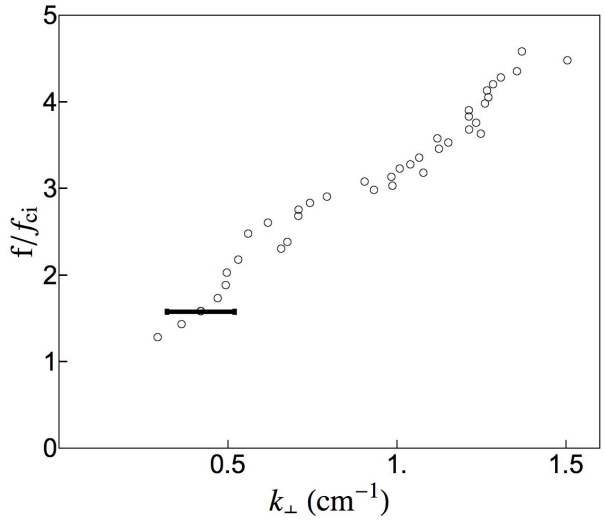

Figure 5. Experimentally determined dispersion relation for the perpendicular component of the wavenumber. A representative error bar is also shown.

D. Choice of BEW frequencies

From Sec. II we found analytically that BEWH is superior to SEWH provided sufficient energy is introduced to the system. For BWX II with its limited power supply, however, it is possible that BEWH may not be the superior process, and the goal of our investigation is to investigate this possibility. In order for BEWH to observe the superiority of BEWH, we require $W_{T(max)}$, the available energy density from our experiment coupled into the waves, to be sufficiently large such that $W_{T(max)} > W_T^*$, where the threshold W_T^* is given by Eq. 7 . Given the limited available power to the waves, in order to have the best chance of seeing the superiority of BEWH heating, we need to identify the frequency combination, ω_1, ω_2 that yields the minimum W_T^*.

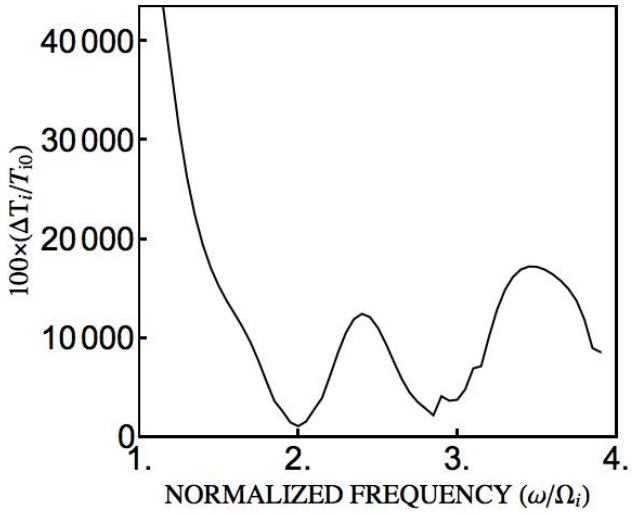

Figure 6. Predicted threshold wave energy density for the superiority of BEWH over SEWH as a function of the frequency in the first mode.

To this end, we use our measured dispersion relation from Fig 5 to plot, in Fig. 6, W_T^* as a function of ω_1 where we have defined $\omega_2 = \omega_1 + \Omega_i$. It is evident from this figure that we expect the lowest required threshold for BEW superiority to occur at the first harmonic $\omega_1 = 2\Omega_i$. We therefore elected to use this frequency combination, $\omega_1 = 2\Omega_i, \omega_2 = 3\Omega_i$, for our experimental investigation.

V. BEW experimental results

For our parametric investigation of BEW heating, we selected the first and second harmonics for our BEW to be $\omega_1 = 2\Omega_i, \omega_2 = 3\Omega_i$. We then analyzed the steady state temperature as a function of the antenna current delivered to each of the two modes. In order to relate this measured current to wave potential amplitude, we generated the calibration curves shown in Fig. 7. These relationships are linear, and we observed the same linear relationship even for the case where the other mode was also present in the plasma.

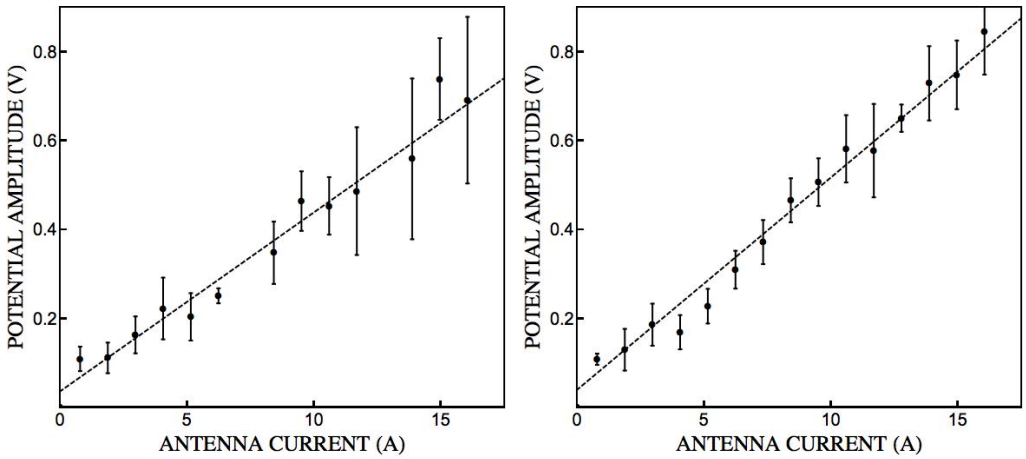

(a) $f = 40$ kHz, $k_\perp = 60$ m^{-1}, and $k_{||} = 50$ m^{-1} (b) $f = 60$ kHz, $k_\perp = 90$ m^{-1}, and $k_{||} = 55$ m^{-1}.

Figure 7. Linear relationship between potential amplitude and antenna current for each of the BEW where $\omega_1 = 2\Omega_i$ in the left plot and $\omega_2 = 3\Omega_i$ in the right plot. The dashed line is a best fit regression.

Armed with this calibration, we were able to infer the potential amplitude for each mode. Then, drawing from the measured dispersion relation in Fig. 5, we could determine the local energy density of each mode. Following this technique, we show in Fig. 8 the percentage increase in ion temperature as a function of the fraction η of wave energy density in the first mode. Each curve corresponds to a different value of total energy density in the two waves, normalized by the analytically predicted threshold value $W_T^* = 3000$ Jm^{-3}. The maximum available energy density we could impart to the plasma with our wave amplifier was only 20% of this threshold value–well below the analytically predicted regime for BEWH superiority. The cases where $\eta \approx 0, 1$ represent SEW heating.

From these results, we identify two classes of behavior. First, for intermediate values of total wave energy density, $0 < W_T < 270$ Jm^{-3}, the scaling of heating efficiency with fractional energy is linear—increasing from $\eta = 0$ to a maximum at $\eta = 1$. This trend reflects the fact that greater absorption occurs for the lower frequency wave ω_1. The slope of this line as well as the intercept at $\eta = 0$ increase with W_T. Second, for higher values of wave energy density, the heating efficiency becomes constant for nearly all fractional combinations of wave energy densities.

The first trend is consistent with our analytical understanding of the BEWH process in the case where the threshold value has not been achieved, $W_T < W_T^*$. In this event, the SEW terms dominate in Eq. 5 such that we anticipate a linear relationship between power absorption (heating efficiency) and the fraction of energy density in the first mode. Indeed, we also can see that this equation predicts the increase in slope and intercept of this linear relationship with total wave energy density. This behavior then is consistent with SEW dominating the power absorption.

There are two possible explanations for the second observed trend with increasing energy density. The first is that we are approaching the limit $W_T = W_T^*$, in which case this plateau is indicative of the emergence of an optimal frequency with $\eta \in (0, 1)$ where BEW is the superior process. The problem with this interpretation is that pursuant to Eq. 6, we would anticipate that with increasing W_T the optimum first will appear near $\eta = 1$ where the individual mode has a higher absorption coefficient and then migrate to $\eta = 1/2$ at higher energy density. The plot indicates, however, that the heating asymptotes near $\eta = 1$.

On the other hand, this observed plateau seems to be more consistent with saturation effects. Indeed, if we still fall in the domain where single wave absorption is the dominant effect $W_T < W_T^*$, we can understand the

profiles shown in Fig. 8 exclusively in terms of the independent single wave absorption of the the propagating modes (the α_j terms). As we have already noted, the temperature increase asymptotes for each combination of waves. If the individual waves are not interacting then, we anticipate that as the total power increases, the power absorption for each wave will saturate. This will occur first at $\eta = 0, 1$, but as the total power increases, each wave will contribute its saturated increase to the temperature for intermediate values of $\eta \in (0, 1)$. For sufficiently large total energy density, this effect will lead to an increasingly uniform profile. The observed plateau therefore seems more consistent with a saturation effect on the individual waves where BEWH represents a negligible contribution.

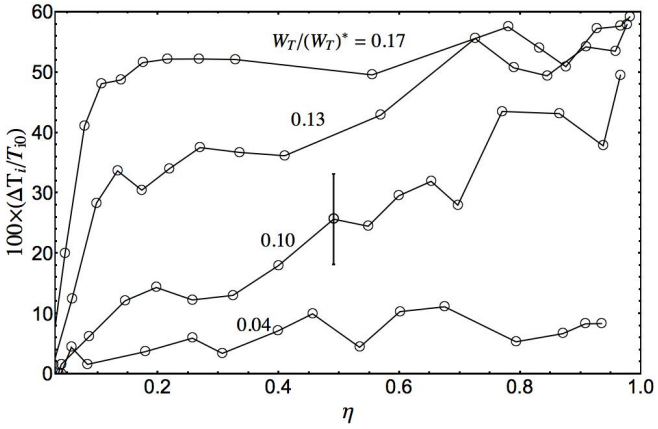

Figure 8. Fractional increase in ion temperature as a function of the fraction of total energy density in the first mode at ω_1. Each curve represents a case where the normalized total wave energy density W_T/W_T^* is constant. $W_T^* = 3000$ $\mathbf{Jm}^{-3}$

VI. Discussion

From our experimental investigation, we have observed even in the optimal configuration where BEWH has the highest likelihood of yielding superior temperature increase, SEWH is the superior process. This is consistent with our calculation of the threshold value W_T^* for BWX II where we have observed that the maximum available energy density in our experiment is below this threshold value. The threshold criteria outlined in Eq. 7 thus is justified and must be taken into consideration when designing a heating scheme.

We should note that our results contradict previously reported investigations of BEWH versus SEWH heating in a plasma similar to the configuration reported here.[20,21] In these results, there was an effort made to control for the same total power to the antenna in both the SEWH and BEWH cases; however, the energy density of the modes propagating in the plasma was not directly measured. The coupling to the plasma from the individual waves thus was not taken into the account–rendering the assumption of equal wave energy density invalid. For example, in the case of BEWH, it is possible that the second introduced mode couples to the plasma more efficiently by virtue of its higher frequency and longer parallel wavenumber. In this event, the total energy introduced into the plasma is greater than the SEWH case–even though the input power from the wave amplifier is the same. It also should be pointed out that these previous investigations examined only a small range of input power values and did not parametrically investigate the effect of fractional content of each mode. Our results presented here are more general.

We finally note that our investigation did not examine the onset of heating for the two cases–though we report on this in another paper.[18] In this low amplitude case, the BEWH effect is in fact superior–another important consideration for experiments with extremely limited available power.

VII. Conclusion

We have presented here a model for power absorption by BEWH and derived a necessary condition for the superiority of BEWH. Even though BEWH is always superior for sufficiently large wave energy densities, there exists a range of lower input values where the heating process favors a single wave. We have investigated

this limit experimentally and found, for the conditions of low temperature and moderate magnetic field of BWX II, SEWH to be the superior hearing process. In this lower bound where SEWH dominates, we have observed the analytically predicted linear dependence on fraction of energy density in the first mode, though saturation effects for power absorption did lead to some unanticipated, but phenomenologically explainable behavior.

In order to exhibit the superiority of BEWH for BWX II, it may be possible to change the plasma parameters to accommodate a lower wave energy density threshold. Alternatively, a new and optimized antenna or higher power sources may be employed. In any event, the results we presented here imply that special care must be taken in applying BEWH to concepts with low temperature plasmas such as plasma propulsion because it is possible that for the given available power, a SEW heating scheme may be preferable.

VIII. Acknowledgements

This material is based upon work supported by the National Science Foundation Graduate Research Fellowship under Grant No. 0646086, the Program in Plasma Science Technology, Princeton Plasma Physics Laboratory, and the NASA Graduate Student Researchers Program.

References

[1]Toki, K., Shinohara, S., Tokai, T., et al., "On the Electrodeless MPD Thruster Using a Compact Helicon Plasma Source," 44th AIAA/ASME/SAE/ASEE Joint Propulsion Conference and Exhibit, Hartford, CT, July 21-23, 2008, No. AIAA-2008-4729, 2008.

[2]Satoh, S., Matsuoka, T., Fujino, T., and Funaki, I., "A Theoretical Analysis for Electrodeless Lissajous Acceleration of HELICON Plasmas," 42nd AIAA Plasmadynamics and Lasers Conference in conjunction with the 18th International Conference on MHD Energy Conversion (ICMHD), Honolulu, Hawaii, June 27-30, 2011, No. AIAA-2011-4008, 2011.

[3]Emsellem, G., "Electrodeless Plasma Thruster Design," 41st AIAA/ASME/SAE/ASEE Joint Propulsion Conference and Exhibit, Tucson, Arizona, July 10-13, 2005, No. AIAA-2005-3855, 2005.

[4]Bering, E. A., Chang-Diaz, F. R., Squire, J. P., Brukardt, M., Glover, T. W., Bengtson, R. D., Jacobson, V. T., McCaskill, G. E., and Cassady, L., "Electromagnetic ion cyclotron resonance heating in the VASIMR," Adv Space Res, Vol. 42, No. 1, Jan 2008, pp. 192–205.

[5]Jorns, B. and Choueiri, E., "A Plasma Propulsion Concept Based on Direct Ion Acceleration with Beating Electrostatic Waves," 46th Joint Propulsion Conference and Exhibit, Nashville, TN, No. AIAA-2010-7107, 2010.

[6]Jorns, B. and Choueiri, E., "Thruster concept for transverse acceleration by the beating electrostatic waves ponderomotive force," 32nd International Electric Propulsion Conference, Wiesbaden, Germany, September 11-15, 2011, No. 214, 2011.

[7]Stix, T., Waves in Plasmas, American Institute of Physics, New York, 1992.

[8]Porkolab, M. and Chang, R. P. H., "Instabilities and Induced Scattering Due to Nonlinear Landau Damping of Longitudinal Plasma Waves in a Magnetic Field," Physics of Fluids, Vol. 15, No. 2, 1972, pp. 283–296.

[9]Ram, A., Bers, A., and Benisti, D., "Ionospheric ion acceleration by multiple electrostatic waves," J. Geophys. Res., Vol. 103, 1998, pp. 9431.

[10]Benisti, D., Ram, A. K., and Bers, A., "Ion dynamics in multiple electrostatic waves in a magnetized plasma. I. Coherent acceleration," Phys. Plasmas, Vol. 5, No. 9, 1998, pp. 3224–3232.

[11]Johnston, S., "Oscillation-center formulation of the classical theory of induced scattering in plasma," Physics of Fluids, Vol. 19, No. 1, 1976, pp. 93–107.

[12]Chang, R. P. H. and Porkolab, M., "Experimental Studies of Nonlinear Landau Damping and Growth of Plasma Waves in a Magnetic Field," Physics of Fluids, Vol. 15, No. 2, 1972, pp. 297–303.

[13]Chia, P.-K., Schmitz, L., and Conn, R., "Stochastic ion behavior in subharmonic and superharmonic electrostatic waves," Phys. Plasmas, Vol. 3, No. 5, May 1996, pp. 1545.

[14]Benisti, D., Ram, A. K., and Bers, A., "Ion dynamics in multiple electrostatic waves in a magnetized plasma. II. Enhancement of the acceleration," Phys. Plasmas, Vol. 5, No. 9, 1998, pp. 3233–3241.

[15]Strozzi, D. J., Ram, A. K., and Bers, A., "Coherent acceleration of magnetized ions by electrostatic waves with arbitrary wavenumbers," Phys. Plasmas, Vol. 10, No. 7, Jul 2003, pp. 2722–2731.

[16]Spektor, R. and Choueiri, E. Y., "Ion acceleration by beating electrostatic waves: Domain of allowed acceleration," Phys. Rev. E, Vol. 69, No. 4, April 2004, pp. 046402.

[17]Jorns, B. and Choueiri, E. Y., "Stochastic ion acceleration by beating electrostatic waves," Submitted for publication.

[18]Jorns, B. and Choueiri, E. Y., "Stochastic threshold for ion heating with beating electrostatic waves," Submitted for publication.

[19]Jorns, B. and Choueiri, E. Y., "Ion Heating with Beating Electrostatic Waves," Phys. Rev. Lett., Vol. 106, No. 8, Feb 2011, pp. 085002.

[20]Spektor, R., Ion Acceleration by Beating Electrostatic Waves, Ph.D Thesis, Princeton University, Princeton, NJ, 2006.

[21]Jorns, B. and Choueiri, E., "Experiment for Plasma Energization with Beating Electrostatic Waves," 31st International Electric Propulsion Conference Proceedings, Ann Arbor, MI, No. 199, 2009.

[22]Sagdeev, R. and Galeev, A., Nonlinear plasma theory, Frontiers in physics, W. A. Benjamin, 1969.

[23]Davidson, R., Methods in Nonlinear Plasma Theory, Academic Press, New York, NY, 1972.

[24]Swanson, D., Plasma Waves, 2nd Edition, Series in Plasma Physics, Taylor & Francis, 2003.

[25]Watson, G., A Treatise on the Theory of Bessel Functions, Cambridge University Press, New York, 1996.

[26]Jorns, B. and Choueiri, E., "Design of an Experiment to Optimize Plasma Energization by Beating Electrostatic Wave," 45th Joint Propulsion Conference and Exhibit, Denver, CO, No. AIAA-2009-5367, 2009.

[27]Light, M. and Chen, F. F., "Helicon wave excitation with helical antennas," Physics of Plasmas, Vol. 2, No. 4, 1995, pp. 1084–1093.

[28]Jorns, B., Sorenson, R., and Choueiri, E., "Variable dual-frequency electrostatic wave launcher for plasma applications," Review of Scientific Instruments, Vol. 82, No. 12, 2011.

[29]Chen, F. and Chang, J., Lecture notes on principles of plasma processing, Kluwer Academic/Plenum Publishers, 2003.

[30]Lieberman, M. A. and Boswell, R. W., "Modeling the transitions from capacitive to inductive to wave-sustained rf discharges," J. Phys. IV France, Vol. 08, 1998, pp. Pr7–145–Pr7–164.

[31]Sarfaty, M., Souza-Machado, S. D., and Skiff, F., "Direct determination of ion wave fields in a hot magnetized and weakly collisional plasma," Physics of Plasmas, Vol. 3, No. 12, 1996, pp. 4316–4324.

[32]Kline, J. L., Scime, E. E., Keiter, P. A., Balkey, M. M., and Boivin, R. F., "Ion heating in the HELIX helicon plasma source," Physics of Plasmas, Vol. 6, No. 12, Dec. 1999, pp. 4767–4772.